Journal of Analytical and Applied Pyrolysis 154 (2021) 104994

Contents lists available at ScienceDirect

Journal of Analytical and Applied Pyrolysis

journal homepage: www.elsevier.com/locate/jaap

Study of rice husk continuous torrefaction as a pretreatment for fast pyrolysis

Olivia Paniz Fleig *, Lucas Manique Raymundo, Luciane Ferreira Trierweiler, Jorge Otávio Trierweiler

Group of Intensification, Modeling, Simulation, Control, and Optimization of Processes (GIMSCOP), Chemical Engineering Department, Federal University of Rio Grande do Sul, Engenheiro Luiz Englert st., Farroupilha, zip code: 90040040, Porto Alegre, RS, Brazil

ARTICLE INFO

Keywords:
Rice husk
Continuous torrefaction
Fast pyrolysis
Bio-oil

ABSTRACT

Rice husk (RH) is one of the most available biomasses in southern Brazil. One possible solution is to carry out the fast pyrolysis of RH. To improve the quality of liquid products biomass can be torrefied before being pyrolyzed. The influence of torrefaction on the physical and chemical properties of pyrolysis products was explored. Both torrefaction and pyrolysis reactions were performed in a fluidized bed reactor in a continuous mode. Sample with torrefaction and pyrolysis at 500 °C presented the highest biochar yield (44.2 wt.%). The torrefaction step produced a lower yield of bio-oil. In contrast, the highest bio-oil yield (43.6 wt.%) was achieved in the sample without torrefaction at 500 °C. The increase in temperature to 750 °C provided a specific area of 16.7 m^2/kg for biochar. The highest value of HHV for bio-oil, 28 MJ/kg, was obtained via direct pyrolysis at 750 °C, which also led to the lowest water content of 5.9 wt%. According to the NMR analysis, the torrefaction liquid (TL) presented a high quantity of water and alcohols in its composition (92.5 %).

1. Introduction

Renewable energy is one of the issues that gain attention, with the increase in the deterioration of the environment and the price of oil. Biomass is an excellent source of renewable energy, it has low cost, abundant reserves, and can be obtained in a short time [1,2]. Except for Asia, Brazil is the largest producer and consumer of rice. About 15 million tons of rice are produced annually in Brazil [3], it is estimated that rice husks (RH) correspond to 20%–34% of this amount [4] The main applications for RH in the industry are in the production of paper, as a source of natural silica, and in the production of cement. One of the most studied applications for rice husks, in the context of renewable energy, is fast pyrolysis [1].

In pyrolysis, biomass is converted into high value-added products, such as bio-oil, biochar, and gas [5,6], which can be used as fuels or chemicals, catalysts or adsorbents, synthesis gas or heating/electricity source, respectively [1,6,7]. However, bio-oil is a liquid with poor fuel qualities, such as high water and oxygen content, acidity, and corrosivity [8]. To improve the quality of bio-oil and allow its applicability, novel pyrolysis processing techniques and pretreatments for biomass are studied [9].

Torrefaction or mild pyrolysis is a thermal pretreatment for biomass, which reaches temperatures between 200 °C and 300 °C and generally in the absence of oxygen [10,11]. It consists primarily of biomass heating in a controlled way to preferably and selectively convert the fraction of biomass that partially grants its low calorific power, such as extractives and polysaccharide compounds mainly from hemicelluloses [12,13]. It is known that torrefaction can improve the fuel properties and grindability of biomass and reduce hydrophilicity [14]. Torrefaction of biomasses promotes an increase in ash and fixed carbon content as well as a reduction in volatile matter content, the latter being the primary source of bio-oil for pyrolysis. From an elementarypoint of view, the main principle of torrefaction is the removal of oxygen from biomass. Besides, torrefaction can effectively decrease the moisture content of biomass, increase its heating value, and decrease the acidity of bio-oil later obtained by pyrolysis (*i.e.* stepwise pyrolysis) [1,15].

From a chemical perspective, the main effects of torrefaction on the lignocellulosic biomass structure are: 1. For cellulose: (i) free hydroxyl groups in the glucose ring are depolymerized from the sugar ring; (ii) the polymer and water-binding regions are reduced, which increases hydrophobic properties; and, (iii) the glycosidic bonds are broken, causing fragmentation of the cellulose structure [16]. 2. For hemicelluloses: (i)

* Corresponding author.
E-mail addresses: oliviapaniz@gmail.com (O.P. Fleig), luciane@enq.ufrgs.br (L.F. Trierweiler).

https://doi.org/10.1016/j.jaap.2020.104994
Received 3 May 2020; Received in revised form 3 December 2020; Accepted 4 December 2020
Available online 22 December 2020

the content of O-acetyl groups decreases considerably, and most of them form acetic acid; and, (ii) methyl groups are decomposed and form gaseous alkenes [17]. 3. For lignin: mainlythe breakdown of ether bonds, which reduces the molar mass of lignin [18].

In most studies in literature, both torrefaction and pyrolysis processes were performed in fixed bed reactors and/or in batches [16]. There are only a few of them addressing reactions in a fluidized bed or a continuous regimen [17,18]. However, no published studies cover torrefaction and pyrolysis using the same equipment with a continuous regime and fluidized bed reactor, as we propose herein.

The schematic flowsheet of torrefaction as pretreatment for pyrolysis is shown in Fig. 1. The objective of this work was to study the effect of rice husk torrefaction on pyrolysis behavior and solid and liquid products of fast pyrolysis. RH was torrefied, and the solid torrefaction product (TS) was then pyrolyzed. For comparison, the pyrolysis of RH was also performed without torrefaction.

2. Materials and methods

2.1. Rice husk

Rice husk (RH) was supplied by Irmãos Moreto Ltda. (Porto Ferreira, SP - Brazil). Before processing, the biomass was milled in a knife mill with 1 mm opening and then sieved to a particle size between 32–80 mesh Tyler. The moisture content of the biomass after milling and sieving was measured as 8.4 wt% on dry basis based on ASTM E871 - 82 (2006).

2.2. Experimental apparatus

The process flow diagram (Fig. 2) describes the laboratory scale equipment used in the experiments. The apparatus comprises a reactor with a fluidized bed and auxiliary equipment. The feeding system is composed of a biomass hopper coupled with a feed auger that determines the feed rate of the feedstock followed by an injection auger that quickly pushes the biomass into the reactor. The feed rate in the feed auger is controlled by means of a variable voltage power supply coupled to a DC motor that drives the mechanism. Initially, the feed auger was calibrated with various voltage values. It was observed that voltage and feed rate had a linear relationship. Biomass feed rate for the experiments was set as 5.2 g/min at 10 V voltage. The fluidized bed reactor is an ASTM304 stainless steel tube with an internal diameter of 22 mm and a length of 350 mm. The heating is made by an electric resistance coupled to the reactor body combined with a liquefied petroleum gas (LPG) burner directly at the base of the reactor. The biochar is separated using two Lapple-type cyclones. Electric resistance is used to heat the two cyclones. A stainless-steel condenser was used to obtain bio-oil. The condenser cooling fluid, a mixture of ethylene glycol and water, was maintained at -8 °C.

The mixture of gases and liquids that were not condensed go to an electrostatic precipitator (EP) that completely captures the aerosols. The EP operates at a voltage of 20 kV DC. The non-condensable gases are exhausted in the environment. The reactor heating system and the LPG flame activation are fully controlled via a programmable logic controller (PLC) and supervised via ELIPSE E3-SCADA system on a computer. The nitrogen injection is controlled by the same PLC. More details about the unit are described elsewhereat [19,20].

2.3. Experimental method

For both torrefaction and pyrolysis, the methodology of the experiment is similar. Before the experiment, the fluidized bed reactor is loaded with 85 g of sand, equivalent to 149 mm of fixed bed height. The sand has a particle size between 40–60 mesh Tyler. RH is loaded into the biomass hopper. The system is heated until the operating temperature is reached (500 °C and 750 °C for pyrolysis or 290 °C for torrefaction). After that, nitrogen is fed to start the fluidization of the bed. Then, the injection auger is turned on as well as the electrostatic precipitator. The experiment starts when the feed auger is turned on, commencing the insertion of biomass into the reactor.

Product quantification is performed after the experiment is done and the system has cooled down. Biochar from the cyclones is collected and weighed. The liquids collected at the condenser and EP are weighed and stored at temperatures between 2 and 4 °C for later analysis.

2.4. Continuous torrefaction

Torrefaction experiments were performed at 290 °C in a continuous regime in the fluidized bed reactor presented in Fig. 2 and previously described. The operating temperature was computer-controlled. Nitrogen was also used as a carrier gas with a flow rate of 1.3 N L/min. RH was fed with a feed rate of 5.2 g/min. The RH particle minimum residence time within the reactor is 1 s. It was determined with the help of a chronometer. At the moment the injection auger was turned on, and biomass started to spread into the reactor, the chronometer was triggered, and at the moment that the first fraction of biochar was visualized in the char catch, the chronometer was stopped. This procedure was repeated three times, and the average time was close to 1 s. The cyclones were kept at 250 °C. The experiments were performed in triplicate, average results are presented. The solid and liquid products of

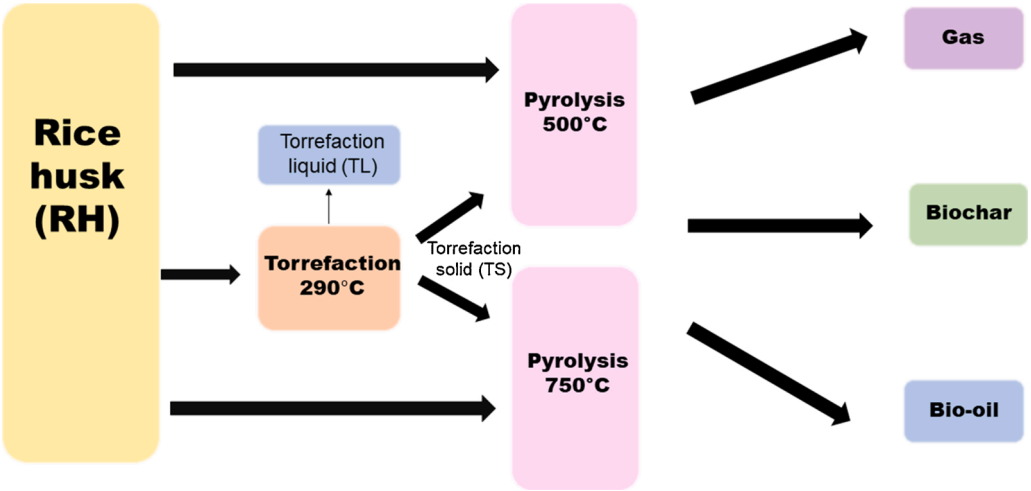

Fig. 1. Schematic flowsheet of torrefaction pretreatment and subsequent fast pyrolysis procedure.

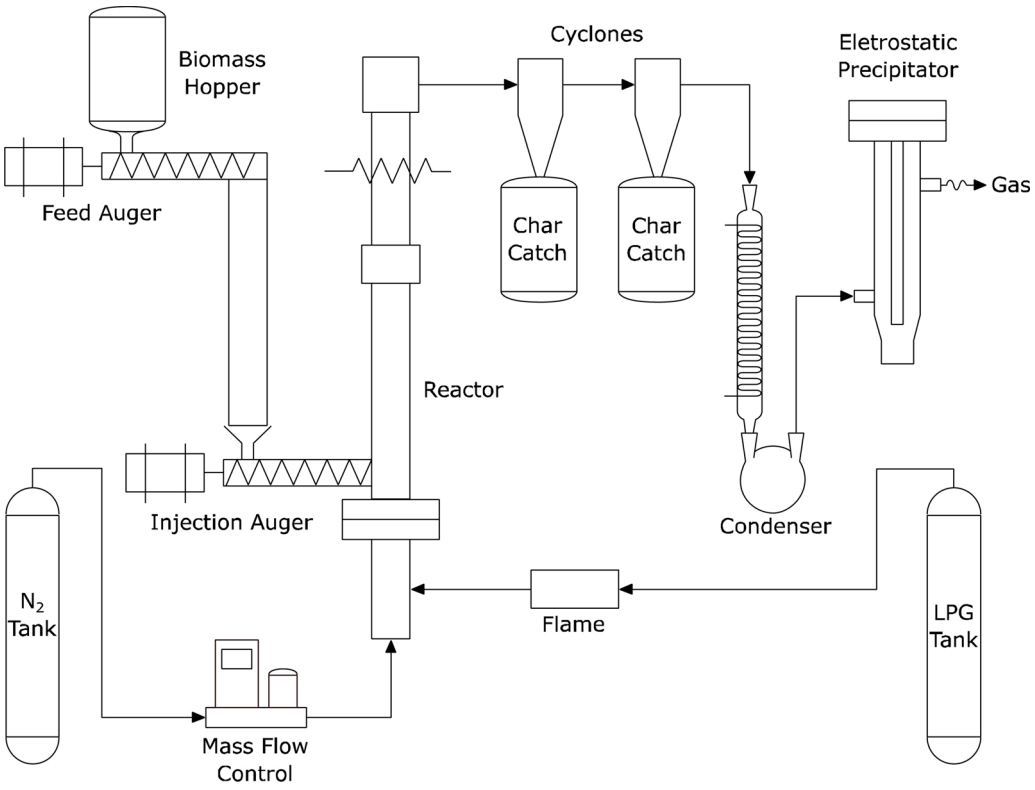

Fig. 2. Process diagram of laboratory scale equipment.

torrefaction are collected and weighed separately.

2.5. Sample identification

Rice husk *in natura* is called RH. The solid product and the liquid product of torrefaction are called TS and TL, respectively. The products of pyrolysis at 500 °C after torrefaction and pyrolysis at 750 °C after torrefaction are denominated P-TS500 and P-TS750, respectively. The products of pyrolysis at 500 °C and 750 °C without torrefaction are denominated P-RH500 and P-RH750, respectively.

2.6. Continuous pyrolysis

Pyrolysis of TS and RH was performed in the same system used for torrefaction. The processing temperatures were 500 °C and 750 °C. The feed rate was 5 g/min. The nitrogen flow rate was 1 N L/min. Cyclones were maintained at 400 °C. Experiments were performed in triplicate, average results are presented. Bio-oil (BO) is the liquid product of pyrolysis, consisting of two fractions, called aqueous phase bio-oil (APBO) and organic phase bio-oil (OPBO). Biochar is the solid product of pyrolysis. Non-condensable gases are called gases. Products were collected and weighed after the pyrolysis experiment. Mass yields of biochar and bio-oil were calculated by weight. Gas yields were calculated by difference.

2.7. Product characterization

Proximate analysis of the solid samples was performed. Ashes are determined based on ASTM E870-82, volatiles are determined by TGA with N_2 as carrier gas (SDT Q600, TA Instruments-Waters, USA) and fixed carbon by difference. The ultimate analysis was performed using an elemental analyzer (CHN SO PE 2400 series II, PerkinElmer, Brazil). Specific surface area (S_{BET}) was determined with surface area analyzers (NOVA 4200e, Quantachrome, Austria). Fourier transform infrared spectroscopy (FTIR) of solid samples was performed on a spectrophotometer (Frontier, PerkinElmer, Brazil). The pH of liquid samples was measured using a digital pHmeter (DM-22, Digimed, Brazil). OPBO and TL sample compositions were analyzed by solution-state proton (1 H) and carbon (13C) NMR spectroscopy recorded on an Avance III Bruker Spectrometer (USA) at 400 MHz. The water content of the liquid samples was determined by the Karl Fischer titration (Q349, Quimis, Brazil). The chemical composition of APBO was determined by High-Performance Liquid Chromatography (HPLC) using an Infinity chromatograph (Agilent, USA) equipped with a Hi Plex H column (Agilent, USA) at 60 °C. Mili-Q water at a flow rate of 0.6 mL/min was used as a mobile phase. The Refractive Index Detector (RID) operated at 55 °C. The run duration was 60 min. With this methodology, glucose, fructose, glycerol, ethanol, methanol, acetic acid, furfural, acetaldehyde, and hydroxymethylfurfural were qualitatively characterized. Higher Heating Value (HHV) of biochar was estimated by elementary composition according to Han [21] using Eq. (1):

$$HHV\ (kJ/kg) = 1.87C^2 - 319C - 1647H + 38.6CH + 133N + 21028 \quad (1)$$

where H, C, N are the mass percentages of hydrogen, carbon, and nitrogen, respectively.

The higher heating value (HHV) of bio-oil was also estimated by the elementary composition according to Han [21] using Eq. (2):

$$HHV\ (MJ/kg) = 0.352C + 0.944H - 0.105O \quad (2)$$

where C, H, O are the mass percentages of carbon, hydrogen, and oxygen, respectively.

3. Results and discussion

3.1. Mass yields of pyrolysis products

The product distribution obtained from the pyrolysis of rice husks, with and without torrefaction, is shown in Table 1.

Using direct fast pyrolysis (P-RH500), the yields of biochar, bio-oil

Table 1
Mass yields of the products of fast pyrolysis.

Product	Sample			
	P-RH500	P-RH750	P-TS500	P-TS750
Biochar	30.5 ± 2.8 ^{bc}	26.2 ± 0.6 ^{c}	44.2 ± 2.2 ^{a}	36.3 ± 1.5 ^{ab}
APBO	33.2 ± 0.8	16.4 ± 3.8 ^{gh}	24 ± 1 ^{g}	15.8 ± 0.7 ^{gh}
OPBO	10.4 ± 0.9 ^{de}	9.7 ± 0.8 ^{def}	11.6 ± 0.2 ^{d}	7.5 ± 0.8 ^{f}
Gases	25.9 ± 2.9 ^{j}	47.7 ± 3.5 ^{i}	20.2 ± 1.4 ^{j}	40.5 ± 1.6 ^{i}

*Averages followed by the same letter do not differ statistically from each other by Tukey's test for each product at 5% probability.

and gases were 30.5 %, 43.6 %, and 25.9 % respectively. Comparing with Chen et al. [22], fast pyrolysis products generated at 500 °C followed the same trend, with the BO as the main product followed by biochar and gases. However, the BO yield obtained by Chen et al. [22] was 53.8 %, and the gas yield was 18.7 %; this difference can be due to the type of reactor and the semi-continuous feed regime used.

The results show that torrefaction caused a 44.9 % increase in P-TS500 biochar yields compared to P-RH500. While BO yields had a 30 % decrease in the P-TS500 sample when compared to P-RH500. One of the reasons for this change is that during torrefaction, biomass is partially decomposed into CO, CO_2, H_2O, and acetic acid [1,23], which reduces the formation of acids and oxygenated compounds during pyrolysis. However, the fraction of organic phase in the BO of P-TS500 is 32.6 %, while for P-RH500 it is 23.8 %. A more substantial amount of organic fraction provides a better quality bio-oil, with a potential decrease in costs of bio-oil refinement. Chen et al. [22] also explored torrefaction at 290 °C, followed by pyrolysis in a semi-continuous quartz reactor. BO yields (33.6 %) were similar to those obtained in this work.

According to Wannapeera et al. [24], Chen et al. [15]], and Chen et al. [22], the observed increase in biochar yield in P-TS500 may have several causes. The first is that torrefaction induces the carbonization of cellulose, leading to the conversion of cellulosic volatile matter into biochar, which also decreases production of bio-oil. Additionally, during torrefaction hemicellulose can be fully decomposed whereas cellulose and lignin are only partially reacted. During the fast pyrolysis of torrefied rice husks, lignin is devolatized to a lesser extent, leading to higher biochar production. Finally the high ash content of rice husks may promote the formation of biochar because they contain several alkaline metals and earthy alkaline metals that catalyze secondary reactions and reduce the production of bio-oil.

Boateng and Mullen [25] confirmed that fast pyrolysis of torrefied biomass produces less bio-oil and more biochar; however, bio-oil from torrefied biomass shows an improvement in some characteristics. Dai et al. [26] state that torrefaction brings to the subsequent pyrolysis process a favoring of cross-linking, increasing the production of biochar and decreasing the production of bio-oil.

It can also be seen that the observed yields at 750 °C were higher for gas, producing little biochar and bio-oil. Alvarez et al. [27] and Chen et al. [28] have demonstrated that the highest production of bio-oil is at temperatures around 500 °C. With increasing temperatures, there is a higher production of gas. Kan et al. [29] state that at temperatures above 600 °C, bio-oil and biochar are converted to gas due to the dominance of secondary cracking reactions.

The ratio of OPBO to APBO should also be taken into account. According to Cen et al. [30], OPBO contains many aromatic compounds that could be used after refining as high added value chemicals instead of being used as fuels, while APBO presents mostly water and acidic compounds. Therefore, it is of great interest to have a higher production of OPBO.

Sample P-RH750 presented the highest proportion of OPBO in relation to APBO, with 59.3 %. It was followed by P-TS500 with 48.3 % and P-TS750, with 47.7 %. On the other hand, P-RH500 had the lowest proportion, of only 31.4 %, distancing itself significantly from the other results. During torrefaction, a large part of the water content of the original biomass is removed, which decreases the production of water in the pyrolysis step and therefore bio-oil water-content. Temperature was also shown to be a factor with a significant influence on water production.

3.2. Biochar

Table 2 shows the properties of RH and pyrolyzed solids. The ash content increased for all samples when compared to the original RH. Pyrolysis increases the ash content due to the decomposition of hemicellulose, cellulose, and lignin that partially leave the solid matrix as volatiles. Torrefied solids (TS) showed the lowest ash content. In comparison, the highest pyrolysis temperature led to the highest ash content in biochar. The most considerable increase in fixed carbon content in P-TS500 is due to the decomposition of cellulose during torrefaction that promotes the carbonization effect, promoting the formation of compounds such as CO, CO_2, and H_2O as well as biochar [16]. Zhang et al. [31] observed that with the increase in pyrolysis temperature, there is an increase in ash content. The carbon content of the samples did not change appreciably except for P-RH750, in which there was a reduction. Carbon is the most desired element when the application of biochar as a solid fuel is sought [1].

The heating value did not show a significant variation between samples *in natura* and pyrolyzed. Charcoal from *Eucalyptus pellita*, which is commercially available as a solid fuel has a HHV in the range of 35 MJ/kg [32]. Comparing the results of HHV obtained in this study and the HHV of *Eucalyptus pellita* coal, it is verified that the biochar of rice husk still has no prospect of being used as solid fuel.

Porosity is one of the crucial factors for biochar, as it influences both burning and adsorption qualities [30]. All samples showed an increase in the specific area when compared to RH. As in Zhang et al. [31], increasing temperatures led to an evident increase in the S_{BET} area, with sample P-CA750 presenting the highest value of 16.7 m^2/g. Torrefaction did not have such a strong influence on S_{BET}, showing that only increasing pyrolysis operation temperatures can promote better surface areas. Biochars with high specific surface areas (>100 m^2/g) can be used as adsorbents or catalysts [15,7].

According to the results of the thermogravimetric analysis, the torrefaction is indeed not able to fully convert cellulose and lignin in the biomass. Torrefied samples (TS) showed proximate and elemental compositions closer to initial RH rather than to the pyrolyzed samples.

3.2.1. TG analysis

Fig. 3 shows the TG curves, and Fig. 4 shows the DTG curves of rice husk (RH), torrefied rice husk (TS), and biochar samples P-RH500, P-RH750, and P-TS500.

The TG analysis shows the loss in mass of the samples with an increase in temperature. At low temperatures, up to 200 °C, small mass losses can be observed, which are related to water evaporation and initial removal of volatiles. Above 200 °C a substantial loss in mass can be seen in TG curves due to the degradation of hemicellulose, cellulose, and lignin. The first peak in the DTG curves corresponds to hemicellulose degradation, and the second peak corresponds to cellulose degradation [15]. For TS, it is possible to observe the disappearance of the first peak due to the conversion of hemicellulose in torrefaction.

In the curves of pyrolyzed samples (P-RH500, P-RH750, and P-TS500), both hemicellulose and cellulose peaks disappear, indicating the thermal degradation of these components. P-RH750 curve is the only one that shows the degradation of lignin fractions in addition to the degradation of hemicellulose and cellulose.

Above 500 °C, the carbonization process is observed where the residues are mainly ashes and fixed carbon [22]. Lignin is the most thermally stable compound, which contributes to the formation of biochar. In contrast, cellulose and hemicellulose contribute to the formation of bio-oil.

Table 2
Properties of rice husk and pyrolyzed solids.

Sample	Proximate analysis (wt.% wb)			Ultimate analysis (wt.% wb)				HHV (MJ/kg)	SBET (m^2/g)
	Volatiles	Fixed carbon	Ash	[C]	[H]	[N]	[O]		
RH	73.9	9	17.10	37.8	5.5	0.3	39.30	15.3	1.5
TS	55.5	17.3	27.2	35.9	4.6	0.7	31.6	15.2	4.2
P-RH500	19.4	31.9	48.7	38.4	2.3	0.3	10.30	16.6	8.5
P-RH750	9.56	32.26	58.2	25.4	1.2	0.4	14.78	16.3	16.7
P-TS500	19.9	36.9	43.2	36.8	2.2	0.5	17.29	16.4	8.4

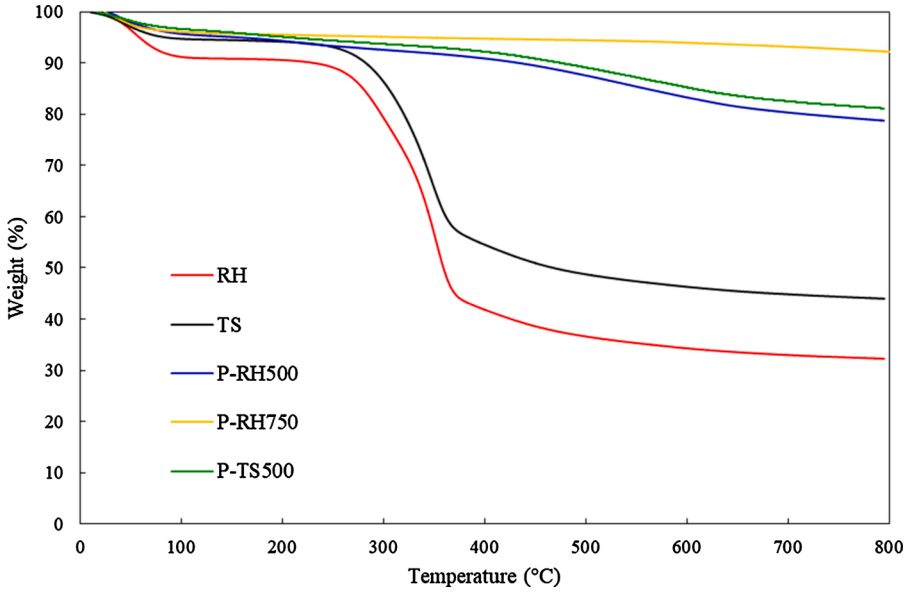

Fig. 3. TG curves of RH, TS, P-RH500, P-RH750, and P-TS500.

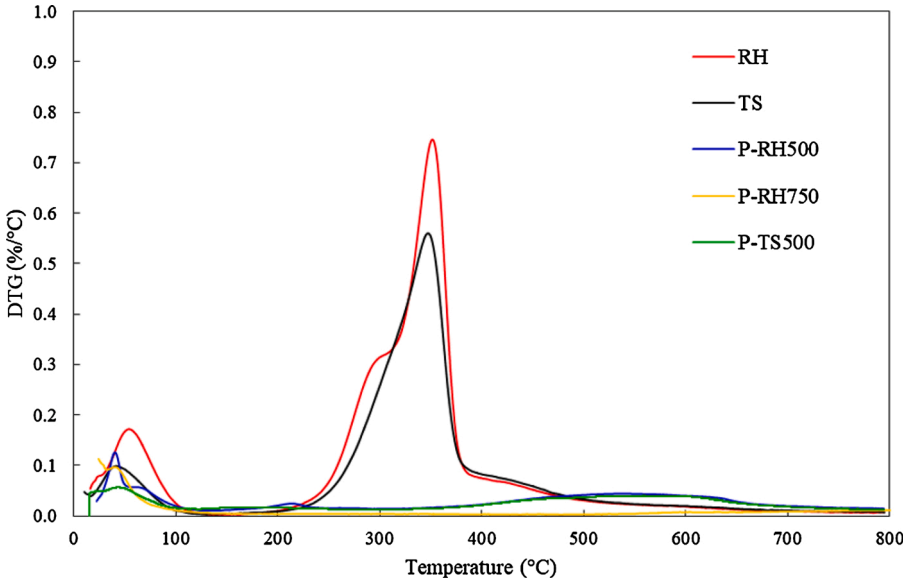

Fig. 4. DTG curves of RH, TS, P-RH500, P-RH750, and P-TS500.

3.2.2. FTIR

The infrared spectra show 7 main bands, as can be seen in Fig. 5. The band with wavenumber between 3600 cm^{-1} and 3200 cm^{-1} is attributed to the vibration of the O—H bond [33], coming from the water contained in the sample [22]. The peak absorbance located between 3000 cm^{-1} and 2700 cm^{-1} is related to the C—H bond [34], indicating the presence of aliphatic hydrocarbons such as CH_4 [2]. The band located close to 1705 cm^{-1} is relative to the CO═ bonds [31] *e.g.* from carboxyl and carbonyl groups. The absorbance peak between 1690 cm $^{-1}$ and 1450 cm^{-1} is from the CC═ bond [22], referring to aromatic moieties. The band between 1500 cm^{-1} and 1200 cm^{-1} is related to CH—$_2$. The band close to 1050 cm^{-1} refers to the SiOS——i bond and,

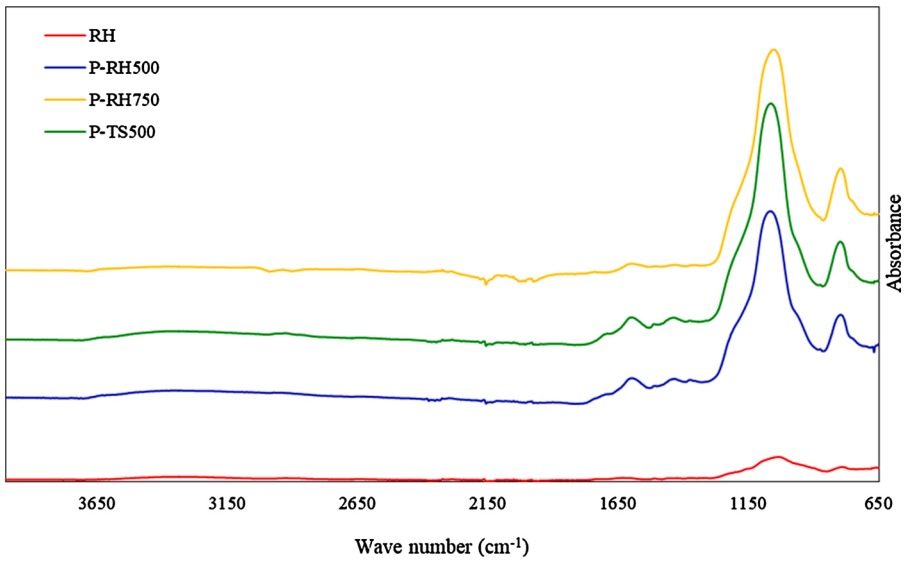

Fig. 5. FTIR spectrum of RH, P-RH500, P-RH750, and P-TS500.

finally, a band close to 780 cm^{-1} refers to the SiO— bond [35].

For all samples, the most notable peaks are Si-O-Si (between 1056 and 1027 cm^{-1}) and SiO (780 $cm^{-}—^{1}$), indicating a high content of silica in the *in natura* husk and biochars. Another point to be observed is that even after heat treatment with torrefaction and at both pyrolysis temperatures, no degradation of silica is apparent.

In the RH sample, the O—H peak close to 3324 cm^{-1} is perceived, indicating that the sample presents a higher water concentration than the others. For the other samples, the intensity of this band is attenuated because all the present moisture has already been removed by the pyrolysis process.

The peak of the C═O bond is more prominent at RH, P-RH500, and P-TS500 than at P-RH750. The increase in temperature, as in the sample P-CA750, may have caused the near disappearance of the C═O peak because, at high temperatures, some functional groups such as carboxyl, carbonyl, and methoxyl can be converted into gaseous or liquid products, leaving the biochar matrix [31].

3.3. Organic phase bio-oil

Table 3 presents the basic properties of the organic phase of bio-oil samples. The sample pre-treated with torrefaction and pyrolyzed at 500 °C (P-TS500) showed the lowest acidity among all samples. Reducing the acidity of bio-oil is critical to make a suitable biofuel intermediate. Chen et al. [36] also measured the pH of BO of torrefied and pyrolyzed samples at the same temperatures applied in this work and obtained a lower pH value, or higher acidity, of 3.0. Both the torrefaction and the temperature have only a small influence on pH since the variation was small. Compared to traditional renewable fuels, such as ethanol, which has a pH between 6 and 8 [37] it can be seen that the increase in pH is far from sufficient for an immediate application as an automotive fuel.

Due to the increased carbon content, the HHV of P-RH750 was 28.1 MJ/kg, while P-RH500 had a HHV of 13.9 MJ/kg and P-TS500 18.5 MJ/kg. Generally, temperatures above 700 °C increase the carbon content of bio-oils in the form of polycyclic aromatic hydrocarbons (PAHs), such as pyrene and phenanthrene, due to decarboxylation and dehydration reactions [29]. Alvarez et al. [27] cite the pyrolysis of lignin as one of the factors to increase the carbon content. This increase corroborates the fact that sample P-RH750 had the highest degradation of lignin in the thermogravimetric analysis.

Chen et al. [36] obtained bio-oils with a HHV of 16.2 MJ/kg when using torrefaction at 290 °C followed by pyrolysis at 500 °C and lower 11.0 MJ/kg when using direct fast pyrolysis at 500 °C. Both results show the same order of magnitude as those obtained in P-TS500 and P-RH500. Comparing the heating value with that of traditional liquid fuels, such as gasoline, diesel, and ethanol, which have a HHV between 23 and 47 MJ/kg [38], it can be seen that only sample P-RH750 has an equivalent HHV.

For a better quality bio-oil, carbon is the desired element, while oxygen is unfavorable [1]. Liquid hydrocarbon-based fuels have an oxygen content close to 1% and a carbon content between 83 and 88 % [39]. P-RH750 presented an oxygen content of 22.3 %, P-TS500 of 43.44 %, and P-RH500 of 56.18 %. The temperature increase was the factor that most affected the results. According to Li et al. [40], pyrolysis bio-oils at high temperatures, between 600 and 900 °C, are considerably less oxygenated due to dehydration, decarbonization, and decarboxylation reactions. This implies a large number of oxygenated functional groups is lost during pyrolysis at high temperatures. Besides, water content is responsible for most of the oxygen content of bio-oils [2], therefore samples with lower water content will present lower oxygen content.

Torrefaction also promoted a decrease in oxygen content when compared to traditional fast pyrolysis at 500 °C. During torrefaction, large amounts of moisture oxygen-rich moieties are removed from biomass, leading to the higher carbon content in bio-oils [1].

Table 3
Basic properties of organic phase bio-oil.

Samples	Ultimate analysis (wt.% wb)				pH	HHV (MJ/kg)	Water content (wt.% wb)
	[C]	[H]	[N]	[O]			
P-RH500	34.1	8.3	1.5	56.2	3	13.9	51.2
P-TS500	50.4	5.6	0.5	43.4	3.5	18.5	37.2
P-RH750	68.6	6.7	2.5	22.3	3.4	28.1	5.9
P-TS750	–	–	–	–	3.17	–	49.2

Water present in the sample is obtained from the initial biomass moisture and dehydration reactions during pyrolysis [27], which are especially significant in hemicellulose decomposition [16]. In this study, temperature was the factor that most affected the water content of bio-oils. P-RH750 showed only 5.9 % water, P-TS500 37.2 %, and P-RH500 51.2 %. Chen, Zhou and Zhang (2014) [22] obtained bio-oils with a water content of 31.7 % under the same conditions as P-TS500.

3.3.1. NMR analysis

Analysis of ^{13}C and ^{1}H OPBO spectra of P-RH500, P-RH750, P-TS500, and P-TS750 are shown in Table 4. In the ^{1}H spectrum for all bio-oil samples, the reduction in alcohol groups from 51.4 % to 16.5 %; 38.0 % and 41.4 % can be observed for P-RH750, P-TS500, and P-TS750 respectively. This reduction was caused by deoxygenation during pyrolysis [41]. For samples P-TS500 and P-TS750, most probably in the torrefaction stage, there is a conversion of alcoholic moieties. This in turn causes a decrease in the percentage of these compounds in bio-oil. All samples showed an increase in aliphatic percentage from 15.6 % (P-RH500) to 27.5 % (P-RH750), 21.7 % (P-TS500) and 18.5 % (P-TS750).

In the ^{13}C spectrum, all bio-oil samples show a significant reduction in the groups: (1) ketones and aldehydes from 2.5 % (P-RH500) to <0.02 % (P-RH750); (2) esters and carboxylic acids from 4.1 % (P-RH500) to 1.0 % (P-RH750); (3) alcohols, ethers, methoxyl and carbohydrates from 22.6 % (P-RH500) to approximately 0.2 % (P-RH750).

Data from both spectra show that deoxygenation results in a reduction in alcohols, ether, carbohydrates, ketones, and aldehydes [41]. Sample P-RH750 showed the most distinct behavior. It showed a high percentage of aromatics for both spectra, 42.5 % for ^{1}H nucleus, and 83.6 % for ^{13}C nucleus. There is also a decrease in long and branched aliphatics from 9.0 % (P-RH500) to 7.5 %, as shown in the ^{13}C spectrum. This decrease indicates that the higher processing temperature has driven the elimination of branching in alkanes. Therefore, the temperature increase promoted a more significant modification in the composition of the organic fraction of the BO than the torrefaction pre-treatment.

3.4. Aqueous phase bio-oil

Table 5 shows the composition of APBO, with the water content and HPLC analytes for each sample. It was not possible to perform a full quantitative analysis by high-efficiency liquid chromatography due to operational problems.

It is possible to see that water is the major component as expected. The organic compounds in APBO are present in small concentrations. Besides the analyzed compounds, no other peaks could be observed in the chromatograms.

The samples processed at 500 °C had a lower water content than the others. Compared to the water content of OPBO, it is visible that these same samples had a higher water content. It may be possible that a higher amount of water-soluble organic compounds is present in APBO generated at 500 °C. Alternatively, water content of OPBO generated at 500 °C is high, therefore it could be essentially extracting water from APBO due to its polarity and oxygen content. There was no significant difference between the APBO of torrefied and non-torrefied biomass generated by pyrolysis at 500 °C.

On the other hand, samples generated at 750 °C showed a significant difference in APBO composition. The traditional fast pyrolysis sample is composed of furfural, ethanol, and methanol. In contrast, the sample with torrefaction showed a single peak, that of glycerol. It is thought that torrefaction was able to separately produce these compounds (furfural, ethanol, and methanol), and thus they were not present in the APBO of sample P-TS750.

Table 4
Percentage of carbon and hydrogen nuclei by signal integration based on 13C NMR and 1H NMR Analysis of Bio-Oils grouped according to chemical shift.

	Chemical shift (ppm)	P-RH500	P-TS500	P-RH750	P-TS750
^{1}H %					
aldehydes	9.5 - 10.1	2.1	2.5	1.6	2.8
aromatics	6.0 - 8.5	14.4	18.3	42.5	19.7
methoxy + carbohydrates	4.4 - 6.0	8.1	7.1	5.2	8.9
alcohol, methylenedibenzene	3.0 - 4.4	51.4	38	16.5	41.4
aliphatics or α- to heteroatom or unsaturation	1.5 - 3.0	15.6	21.7	27.5	18.5
alkanes	0.5 - 1.5	8.3	12.4	6.7	8.6
^{13}C %					
ketones, aldehydes	180 - 215	2.5	1.85	0	1.3
esters, carboxylic acids	165 - 180	4.1	3.2	1	2.7
aromatics, olefins	95 - 165	45.5	55.3	83.6	60
alcohols, ethers, phenolicmethoxy, carbohydrates	55 - 95	22.6	13.3	0.2	14.5
long and branched aliphatics	28 - 55	9	10.95	7.5	11
short aliphatics	0 - 28	16.3	15.4	7.7	10.5

3.5. Liquid product of torrefaction

Table 6 shows the water content, pH value, and analyses of the ^{1}H and ^{13}C NMR spectra of the liquid product produced during torrefaction.

The TL sample presents mostly water in its composition (83.7 %) and 92.5 % of alcohol moieties in the organics by analysis of NMR of ^{1}H. Concurring with what was commented in the previous OPBO NMR analysis, that the OPBO samples pre-treated by torrefaction presented a lower content of alcohols, these compounds are formed during torrefaction and remain in the TL, thus are not present in large quantities in the later generated bio-oil. The formation of these compounds during torrefaction is due to the degradation of hemicellulose. Comparing the ^{1}H nucleus spectrum with Raymundo et al. [41], Biswas et al. [42], and Mullen et al. (2009), the hypothesis is that the main compound formed in the TL is methanol.

4. Conclusions

The primary changes observed by torrefaction pre-treatment and high temperature pyrolysis were in the distribution of solid, liquid, and gaseous products. The fuel properties of bio-oil were improved by processing at 750 °C, with an HHV of 28.1 MJ/kg for OPBO. The temperature of 750 °C also led to the highest value of S_{BET} and pore size of the biochar samples. ^{1}H NMR analysis of the samples showed high alcohol contents for TL, while fast pyrolysis at 750 °C led to a significant presence of aromatics in OPBO. In general, both torrefaction pre-treatment followed by pyrolysis at 500 °C and the direct pyrolysis of rice husks at 750 °C have shown to increase HHV and reduce acidity of OPBO, where the higher temperature pyrolysis had a more significant effect. Bio-oils obtained with these techniques could therefore be more suitable as chemical and fuel precursors.

Author statement

Jorge Trierweiler and Luciane Trierweiler conceived of the presented idea. Lucas Raymundo and Olivia Fleig developed the experimental methods, carried out the experiment and analysis. Jorge and Luciane supervised the findings of this work. All authors discussed the results and contributed to the final manuscript.

Funding

This work was supported by the Coordenação de Aperfeiçoamento de

Table 5
Water content and composition of APBO.

Sample	Water content (wt.%)	Composition
P-RH500	49.5	Glycerol, acetic acid, methanol, furfural, 5-HMF
P-TS500	51.1	Glycerol, acetic acid, furfural, methanol
P-RH750	74.1	Methanol, furfural, ethanol
P-TS750	60.3	Glycerol

Table 6
Water content, pH, and percentage of hydrogen and carbon nuclei based on ^{1}H NMR and ^{13}C NMR of TL.

Analysis		TL
Water content (wt.%)		83.7
pH		2.6
Groups	Chemical shift (ppm)	
^{1}H (%)		
aldehydes	9.5 - 10.1	0.1
aromatics	6.0 - 8.5	0.4
methoxy + carbohydrates	4.4 - 6.0	0.9
alcohol, methylenedibenzene	3.0 - 4.4	92.5
aliphatics or α- to heteroatom or unsaturation	1.5 - 3.0	4.9
alkanes	0.5 - 1.5	1.2
^{13}C (%)		
ketones, aldehydes	180 - 215	2.6
esters, carboxylic acids	165 - 180	13
aromatics, olefins	95 - 165	9.1
alcohols, ethers, phenolic methoxy, carbohydrates	55 - 95	17.6
long and branched aliphatics	28 - 55	27.1
short aliphatics	0 - 28	30.6

Pessoal de Nível Superior (CAPES).

Declaration of Competing Interest

The authors report no declarations of interest.

Acknowledgements

To the Magnetic Resonance Laboratory of UFRGS for the support in the development of the NMR analysis contained in this work.

References

[1] L. Dai, Y. Wang, Y. Liu, R. Ruan, C. He, Z. Yu, L. Jiang, Z. Zeng, X. Tian, Integrated process of lignocellulosic biomass torrefaction and pyrolysis for upgrading bio-oil production: a state-of-the-art review, Renewable Sustainable Energy Rev. 107 (2019) 20–36, https://doi.org/10.1016/j.rser.2019.02.015.
[2] P.K. Kanaujia, Y.K. Sharma, M.O. Garg, D. Tripathi, R. Singh, Review of analytical strategies in the production and upgrading of bio-oils derived from lignocellulosic biomass, J. Anal. Appl. Pyrolysis 105 (2014) 55–74, https://doi.org/10.1016/j.jaap.2013.10.004.
[3] Brazilian Rice, (n.d.). http://brazilianrice.com.br/en/. (Accessed 27 September 2019).
[4] L.P. Fontoura, Portencial Econômico e Aplicações da Casca de Arroz no Estado do Rio Grande do Sul, Universidade Federal do Rio Grande do Sul, 2015.
[5] S. Zhang, Y. Su, K. Ding, S. Zhu, H. Zhang, X. Liu, Y. Xiong, Effect of inorganic species on torrefaction process and product properties of rice husk, Bioresour. Technol. 265 (2018) 450–455, https://doi.org/10.1016/j.biortech.2018.06.042.
[6] P. Basu, Biomass Gasification and Pyrolysis, 2010, https://doi.org/10.1016/C2009-0-20099-7.
[7] F.R. Oliveira, A.K. Patel, D.P. Jaisi, S. Adhikari, H. Lu, S.K. Khanal, Environmental application of biochar: current status and perspectives, Bioresour. Technol. 246 (2017) 1–282, https://doi.org/10.1016/j.biortech.2017.08.122. In press.
[8] N. Worasuwannarak, T. Sonobe, W. Tanthapanichakoon, Pyrolysis behaviors of rice straw, rice husk, and corncob by TG-MS technique, J. Anal. Appl. Pyrolysis 78 (2007) 265–271, https://doi.org/10.1016/j.jaap.2006.08.002.
[9] D. Carpenter, T.L. Westover, S. Czernik, W. Jablonski, Biomass feedstocks for renewable fuel production: a review of the impacts of feedstock and pretreatment on the yield and product distribution of fast pyrolysis bio-oils and vapors, Green Chem. 16 (2) (2014) 367–926, https://doi.org/10.1039/c3gc41631c.
[10] K.Q. Tran, X. Luo, G. Seisenbaeva, R. Jirjis, Stump torrefaction for bioenergy application, Appl. Energy 112 (2013) 1–1566, https://doi.org/10.1016/j.apenergy.2012.12.053.
[11] T.A. Mamvura, G. Danha, Biomass torrefaction as an emerging technology to aid in energy production, Heliyon 6 (3) (2020), https://doi.org/10.1016/j.heliyon.2020.e03531.
[12] C.M.S. da Silva, A. de C.O. Carneiro, B.R. Vital, C.G. Figueiró, L. de F. Fialho, M. A. de Magalhães, A.G. Carvalho, W.L. Cândido, Biomass torrefaction for energy purposes – definitions and an overview of challenges and opportunities in Brazil, Renewable Sustainable Energy Rev. 82 (2018) 2426–2432, https://doi.org/10.1016/j.rser.2017.08.095.
[13] W.H. Chen, C.W. Wang, H.C. Ong, P.L. Show, T.H. Hsieh, Torrefaction, pyrolysis and two-stage thermodegradation of hemicellulose, cellulose and lignin, Fuel 258 (2019), https://doi.org/10.1016/j.fuel.2019.116168.
[14] S. Zhang, Q. Dong, T. Chen, Y. Xiong, Combination of light bio-oil washing and torrefaction pretreatment of rice husk: its effects on physicochemical characteristics and fast pyrolysis behavior, Energy Fuels 30 (2016) 3030–3037, https://doi.org/10.1021/acs.energyfuels.5b02968.
[15] D. Chen, K. Cen, X. Jing, J. Gao, C. Li, Z. Ma, An approach for upgrading biomass and pyrolysis product quality using a combination of aqueous phase bio-oil washing and torrefaction pretreatment, Bioresour. Technol. 233 (2017) 150–158, https://doi.org/10.1016/j.biortech.2017.02.120.
[16] D. Chen, A. Gao, Z. Ma, D. Fei, Y. Chang, C. Shen, In-depth study of rice husk torrefaction: characterization of solid, liquid and gaseous products, oxygen migration and energy yield, Bioresour. Technol. 253 (2018) 148–153, https://doi.org/10.1016/j.biortech.2018.01.009.
[17] A. Kulkarni, R. Baker, N. Abdoulmomine, S. Adhikari, S. Bhavnani, Experimental study of torrefied pine as a gasification fuel using a bubbling fluidized bed gasifier, Renew. Energy 93 (2016) 1–708, https://doi.org/10.1016/j.renene.2016.03.006.
[18] H. Li, X. Liu, R. Legros, X.T. Bi, C.J. Lim, S. Sokhansanj, Torrefaction of sawdust in a fluidized bed reactor, Bioresour. Technol. 103 (1) (2012) 1–502, https://doi.org/10.1016/j.biortech.2011.10.009.
[19] L.M. Raymundo, J.S. Espindola, F.C. Borges, E. Lazzari, J.O. Trierweiler, L. F. Trierweiler, Continuous fast pyrolysis of rice husk in a fluidized bed reactor with high feed rates, Chem. Eng. Commun. 207 (2020), https://doi.org/10.1080/00986445.2020.1798937.
[20] L.M. Raymundo, Desenvolvimento De Uma Planta Laboratorial De Pirólise Rápida Em Leito Fludizado Aplicado À Casca De Arroz, 2016, p. 125. https://www.lume.ufrgs.br/bitstream/handle/10183/148012/001001335.pdf?sequence=1.
[21] Z. Han, X. Zeng, C. Yao, G. Xu, Oxygen Migration in Torrefaction of Eupatorium adenophorum Spreng and Its Improvement on Fuel Properties, 2015, https://doi.org/10.1021/acs.energyfuels.5b01318.
[22] D. Chen, J. Zhou, Q. Zhang, Effects of torrefaction on the pyrolysis behavior and bio-oil properties of rice husk by using TG-FTIR and Py-GC/MS, Energy Fuels 28 (2014) 5857–5863, https://doi.org/10.1021/ef501189p.
[23] H. Persson, T. Han, L. Sandström, W. Xia, P. Evangelopoulos, W. Yang, Fractionation of liquid products from pyrolysis of lignocellulosic biomass by stepwise thermal treatment, Energy 154 (2018) 346–351, https://doi.org/10.1016/j.energy.2018.04.150.
[24] J. Wannapeera, B. Fungtammasan, N. Worasuwannarak, Effects of temperature and holding time during torrefaction on the pyrolysis behaviors of woody biomass, J. Anal, Appl. Pyrolysis 92 (1) (2011) 99–105, https://doi.org/10.1016/j.jaap.2011.04.010.
[25] A.A. Boateng, C.A. Mullen, Fast pyrolysis of biomass thermally pretreated by torrefaction, J. Anal. Appl. Pyrolysis 100 (2013) 95–102, https://doi.org/10.1016/j.jaap.2012.12.002.
[26] L. Dai, Y. Wang, Y. Liu, R. Ruan, C. He, Z. Yu, L. Jiang, Z. Zeng, X. Tian, Integrated process of lignocellulosic biomass torrefaction and pyrolysis for upgrading bio-oil production: a state-of-the-art review, Renew. Sustain. Energy Rev. 107 (2019) 20–36, https://doi.org/10.1016/j.rser.2019.02.015.
[27] J. Alvarez, G. Lopez, M. Amutio, J. Bilbao, M. Olazar, Bio-Oil Production from Rice Husk Fast Pyrolysis in a Conical Spouted Bed Reactor, 2014.
[28] D. Chen, Y. Li, K. Cen, M. Luo, H. Li, B. Lu, Pyrolysis polygeneration of poplar wood : Effect of heating rate and pyrolysis temperature, Bioresour. Technol. 218 (2016) 780–788.

[29] T. Kan, V. Strezov, T.J. Evans, Lignocellulosic biomass pyrolysis: a review of product properties and effects of pyrolysis parameters, Renew. Sustain. Energy Rev. 57 (2016) 1126–1140, https://doi.org/10.1016/j.rser.2015.12.185.
[30] K. Cen, J. Zhang, Z. Ma, D. Chen, J. Zhou, H. Ma, Investigation of the relevance between biomass pyrolysis polygeneration and washing pretreatment under different severities: water, dilute acid solution and aqueous phase bio-oil, Bioresour. Technol. 278 (2019) 26–33, https://doi.org/10.1016/j.biortech.2019.01.048.
[31] Y. Zhang, Z. Ma, Q. Zhang, J. Wang, Q. Ma, Y. Yang, X. Luo, W. Zhang, Comparison of the physicochemical characteristics of bio-char pyrolyzed from moso bamboo and rice husk with different pyrolysis temperatures, BioResources 12 (2017) 4652–4669, https://doi.org/10.15376/biores.12.3.4652-4669.
[32] A.C. Oliveira, A.C.O. De Carneiro, B.R. Vital, W. Almeida, B.L.C. Pereira, M. T. Cardoso, Parâmetros de qualidade da madeira e do carvão vegetal de Eucalyptus pellita F. Muell, Sci. For. Sci. (2010) 431–439.
[33] Z. Ma, D. Chen, J. Gu, B. Bao, Q. Zhang, Determination of pyrolysis characteristics and kinetics of palm kernel shell using TGA-FTIR and model-free integral methods, Energy Convers. Manage. 89 (1) (2015) 251–259, https://doi.org/10.1016/j.enconman.2014.09.074.
[34] Z. Ma, Q. Sun, J. Ye, Q. Yao, C. Zhao, Study on the thermal degradation behaviors and kinetics of alkali lignin for production of phenolic-rich bio-oil using TGA-FTIR and Py-GC/MS, J. Anal. Appl. Pyrolysis 117 (2016) 1–370, https://doi.org/10.1016/j.jaap.2015.12.007.
[35] S. Zhang, Q. Dong, T. Chen, Y. Xiong, Combination of light bio-oil washing and torrefaction pretreatment of rice husk: its effects on physicochemical characteristics and fast pyrolysis behavior, Energy Fuels 30 (2016) 3030–3037, https://doi.org/10.1021/acs.energyfuels.5b02968.
[36] D. Chen, J. Zhou, Q. Zhang, X. Zhu, Q. Lu, Upgrading of rice husk by torrefaction and its influence on the fuel properties, BioResources 9 (2014) 5893–5905, https://doi.org/10.15376/biores.9.4.5893-5905.
[37] ANP, (n.d.). http://legislacao.anp.gov.br. (Accessed 30 September 2019).
[38] Heat Values of Various Fuels, (n.d.). https://www.world-nuclear.org/information-library/facts-and-figures/heat-values-of-various-fuels.aspx. (Accessed 30 September 2019).
[39] O.P. Gupta, Elements of Fuels, Furnaces & Refractories No Title, 6th ed., KHANNA Publishers, 1989.
[40] J. Li, R. Yan, B. Xiao, X. Wang, H. Yang, V. Uni, N.D. V, V. Recei, V. No, V. Re, M. Recei, V. May, Influence of Temperature on the Formation of Oil from Pyrolyzing Palm Oil Wastes in a Fixed Bed Reactor, 1, 2007, pp. 2398–2407.
[41] L.M. Raymundo, C.A. Mullen, G.D. Strahan, A.A. Boateng, J.O. Trierweiler, Deoxygenation of biomass pyrolysis vapors via in situ and ex situ thermal and biochar promoted upgrading, Energy Fuels 33 (2019) 2197–2207, https://doi.org/10.1021/acs.energyfuels.8b03281.
[42] B. Biswas, N. Pandey, Y. Bisht, R. Singh, J. Kumar, T. Bhaskar, Pyrolysis of agricultural biomass residues: comparative study of corn cob, wheat straw, rice straw and rice husk, Bioresour. Technol. 237 (2017) 57–63, https://doi.org/10.1016/j.biortech.2017.02.046.